Supplementary information

Selective sensing of *aliphatic* biogenic polyamines by zwitterionic Cd-MOF based on bisimidazole tetracarboxylic acid linker

Swati Jindal,[a] Vijay Kumar Maka,[a] and Jarugu Narasimha Moorthy*[ab]

[a]*Department of Chemistry, Indian Institute of Technology, Kanpur 208016, INDIA*
[b]*School of Chemistry, Indian Institute of Science Education and Research Thiruvananthapuram 695551, INDIA*

*Corresponding Author; E-mail: moorthy@iitk.ac.in

Contents

1.	Syntheses and characterization of diketodiester **1**	S2
2.	Crystal data and refinement parameters for **Cd-BBI**	S3
3.	PXRD profile of **Cd-BBI**	S4
4.	TGA profile of **Cd-BBI**, and FT-IR profiles of **H_4BBI** and **Cd-BBI**	S4
5.	Quenching of the fluorescence of **Cd-BBI** with increasing concentration of analyte (*n*-PA, DIPA, TEA and Aniline) in EtOH	S5-S7
6.	Quenching of the fluorescence of tetraester **2** with increasing concentration of DIPA in EtOH	S7
7.	Quenching of the fluorescence of **Cd-BBI** with increasing concentration of amine (His, TYA and TPA) in EtOH and determination of the Stern–Volmer quenching constant	S8-S9
8.	Time-resolved fluorescence quenching titration of **Cd-BBI** with increasing concentration of SPM in EtOH and linear plot of (τ_0/τ) versus concentration of SPM	S9
9.	Fluorescence lifetime decay data of **Cd-BBI** with the addition of SPM	S10
10.	Quenching of the fluorescence of **H_4BBI** with increasing concentration of amine (SPM, SPD, His, TYA and TPA) in EtOH and determination of the Stern–Volmer quenching constant	S10-S12
11.	Time-resolved fluorescence decay trace of **H_4BBI** in EtOH recorded using TCSPC	S13
12.	Fluorescence quenching data of **H_4BBI** for various biogenic amines in EtOH	S13
13.	Determination of the sensitivity limit of **Cd-BBI** for detection of SPM	S14
14.	Comparison of sensing properties of **Cd-BBI** MOF with different SPM optical probes	S15
15.	References	S16
16.	^{1}H and ^{13}C NMR spectra of compounds	S17-S19

Synthesis of dimethyl 4,4-oxalyldibenzoate (1)

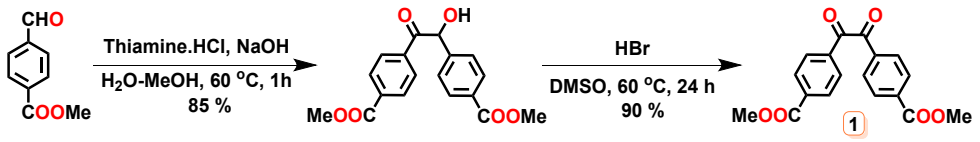

A 25 mL round-bottomed flask was charged with thiamine•HCl (0.185 g, 0.55 mmol) and 2 mL of H_2O/MeOH (1:3), and the solution was cooled down using an ice-bath. Subsequently, addition 0.5 mL of 2 M NaOH solution was introduced slowly over a period of 10 min followed by 4-formylbenzoate (1.5 g, 9.14 mmol), and the contents were heated at reflux for 1 h. After completion of the reaction, the reaction mixture was cooled down to rt, and the resultant precipitate was filtered. The filtered solid material was washed with cold MeOH and dried under vacuum to afford dimethyl 4,4'-(2-hydroxyacetyl)dibenzoate[1] as an off-white solid in 85 % yield, (1.28 g); ^{1}H NMR (400 MHz, $CDCl_3$) δ 3.86 (s, 3H), 3.9 (s, 3H), 6.0 (d, J = 6 Hz, 1H), 7.39 (d, J = 8 Hz, 2H), 7.92 (d, J = 8 Hz, 2H), 8.04 (d, J = 8.4 Hz, 2H).

A 25 mL round bottom flask was charged with dimethyl 4,4'-(2-hydroxyacetyl)dibenzoate (1.5 g, 4.56 mmol), DMSO (5 mL) and 40% aqueous HBr (1 mL). The resultant mixture was heated to 60 °C for 12 h. After completion of the reaction, the reaction mixture was cooled down to rt and poured into ice-cold water. The yellow-colored precipitate formed was filtered, thoroughly washed with water and dried. The crude compound was recrystallized from MeOH to obtain diketodiester **1** as a yellow-colored solid in 90% yield (1.35 g); ^{1}H NMR (400 MHz, $CDCl_3$) δ 3.96 (s, 6H), 8.05 (d, J = 8.4 Hz, 4H), 8.18 (d, J = 8.8 Hz, 4H).

Table S1 Crystal data and refinement parameters for **Cd-BBI**.

Identification code	**Cd-BBI**
Empirical formula	$C_{44}H_{24}CdN_4O_8$
Formula weight	801.04
Temperature (K)	100
Wavelength (Å)	0.71073
Crystal system	monoclinic
Space group	C2/c
a (Å)	20.0809(10)
b (Å)	18.6869(10)
c (Å)	13.6347(7)
α (deg)	90
β (deg)	103.484(2)
γ (deg)	90
Volume (Å^3)	4975.4(4)
Z	4
Density (calculated) (mg/m^3)	1.069
Absorption coefficient (mm^{-1})	0.482
F(000)	1616.0
2θ range for data collection (°)	6.036 to 56.562°
Index ranges	$-26 \leq h \leq 26$
	$-24 \leq k \leq 24$
	$-18 \leq l \leq 18$
Reflections collected	53002
Independent reflections	6159 [R_{int} = 0.0332
	R_{sigma} = 0.0176]
Completeness to theta = 25.242°	100 %
Absorption correction	None
Refinement method	Full-matrix least-squares on F^2
Data / restraints / parameters	6159/0/216
Goodness-of-fit on F^2	1.039
Final R indices [I>2sigma(I)]	R_1 = 0.0611, wR_2 = 0.1706
Final R indices (all data)	R_1 = 0.0640, wR_2 = 0.1744
Largest diff. peak and hole	2.6 and -2.3 eÅ^{-3}
CCDC deposition number	1975342

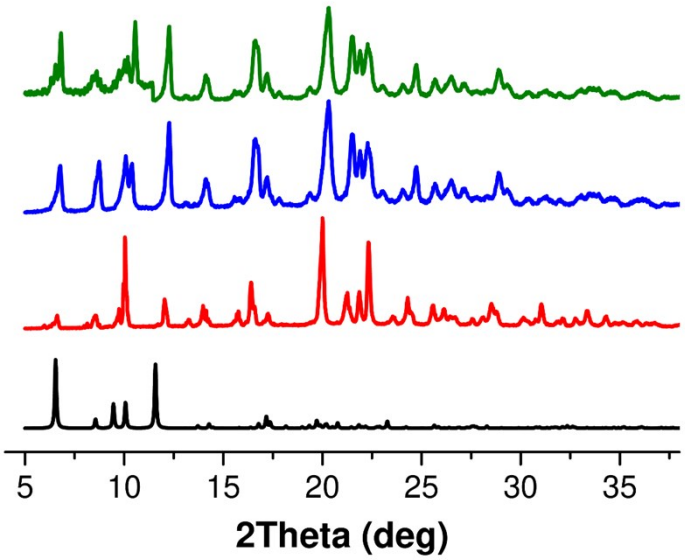

Fig. S1 PXRD profiles of **Cd-BBI**: simulated for the X-ray determined single crystal structure (black), pristine MOF crystals synthesized in bulk (red) and MOF crystals immersed in 0.5 mM of SPM (blue) and SPD (green) solutions for 1 h.

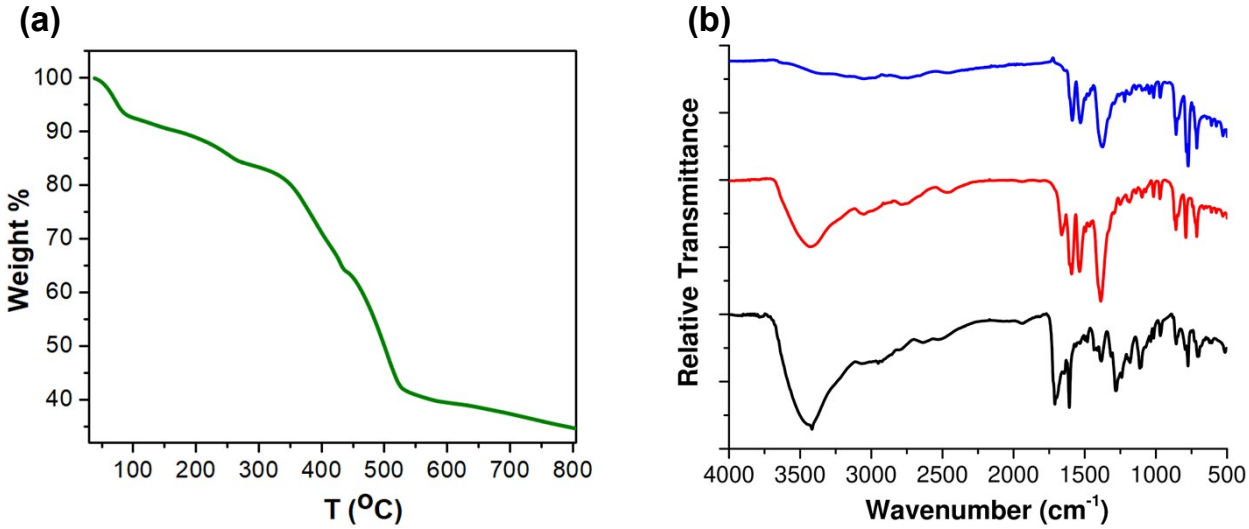

Fig. S2 (a) TGA profile of **Cd-BBI**. (b) FT-IR profile of **H_4BBI** (black line), **Cd-BBI** (red line), and **Cd-BBI** with SPM (blue line).

Steady-state fluorescence spectroscopy experiments

The steady-state fluorescence measurements were carried out on a FluoroMax-4 spectrofluorometer (Horiba Jobin Yvon Technology) with an accuracy of ± 1 nm.

The fluorescence quenching experiments on tetraester 2 were performed using 1 μM solution in DMF with incremental addition of DIPA (0.5 mM in EtOH) for λ_{ex} = 370 nm. The steady-state fluorescence quenching experiments on **H_4BBI** (1 μM) in EtOH were carried out by the incremental addition of the amine. Stern-Volmer quenching constants (K_{SV}s) were calculated by linear regression analysis.

For the steady-state fluorescence quenching studies on Cd-MOF, the MOF suspension was prepared by sonication of 10 mg of MOF in EtOH (10 mL) for 30 min. Fluorescence quenching titrations (λ_{ex} = 370 nm) were carried out by incremental addition of the ethanolic solution of amine.

The equation that defines fluorescence quenching efficiency (%) as follows:

$$\eta = \left[\frac{I_0 - I}{I_0}\right] \times 100\ \%$$

Time-resolved fluorescence quenching titration experiment with Cd-BBI

Time-resolved fluorescence decays were recorded on time-correlated single-photon counting instrument (Fluorolog, Horiba Jobin Yvon) using a nanosecond pulsed diode laser (λ_{ex} = 340 nm) at rt. The instrument response function (IRF) was measured by using LUDOX as the scatterer and the decay in each case was fitted by using a reconvolution software supplied with the instrument. The dynamic/static nature of fluorescence quenching of **Cd-BBI** by the biogenic amine was established by time-resolved fluorescence quenching titration with SPM as a representative analyte. Accordingly, the MOF suspension was placed in a quartz cell of 1 cm in width. The fluorescence quenching titrations were carried out by incremental addition of SPM to the suspension of **Cd-BBI**, and the time-resolved fluorescence decays of **Cd-BBI** were recorded at rt for excitation at 340 nm. The singlet lifetime (τ_{avg}) of **Cd-BBI** was, therefore, determined after each addition of the analyte. The biexponential fitting of the decay in each case was fitted with the goodness of fit χ^2 being close to 1, cf. Table S2.

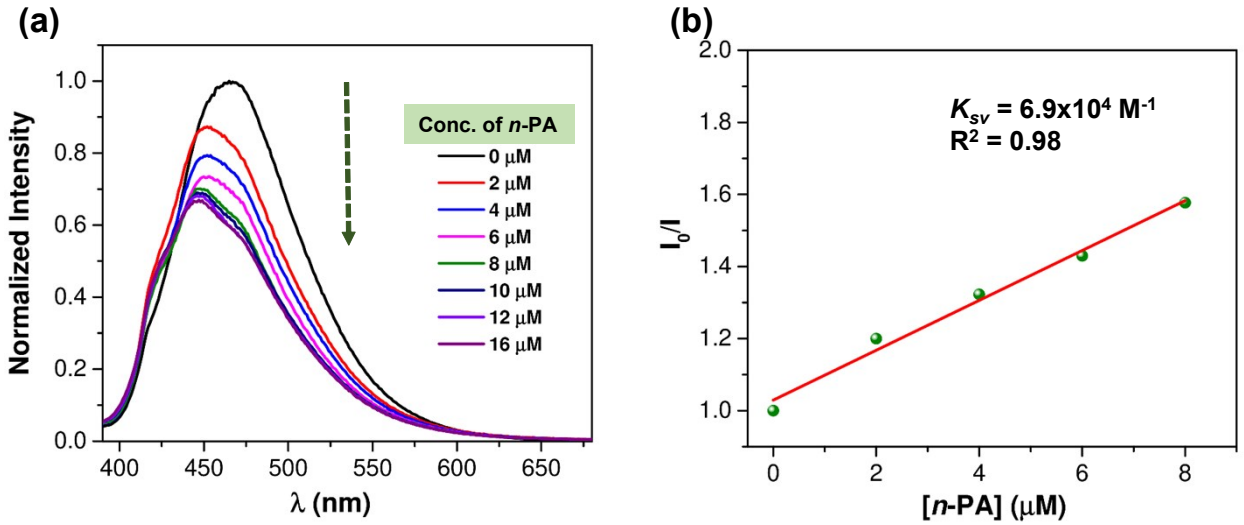

Fig. S3 (a) Quenching of the fluorescence of **Cd-BBI** with increasing concentration of *n*-PA. (b) Determination of the Stern–Volmer quenching constant.

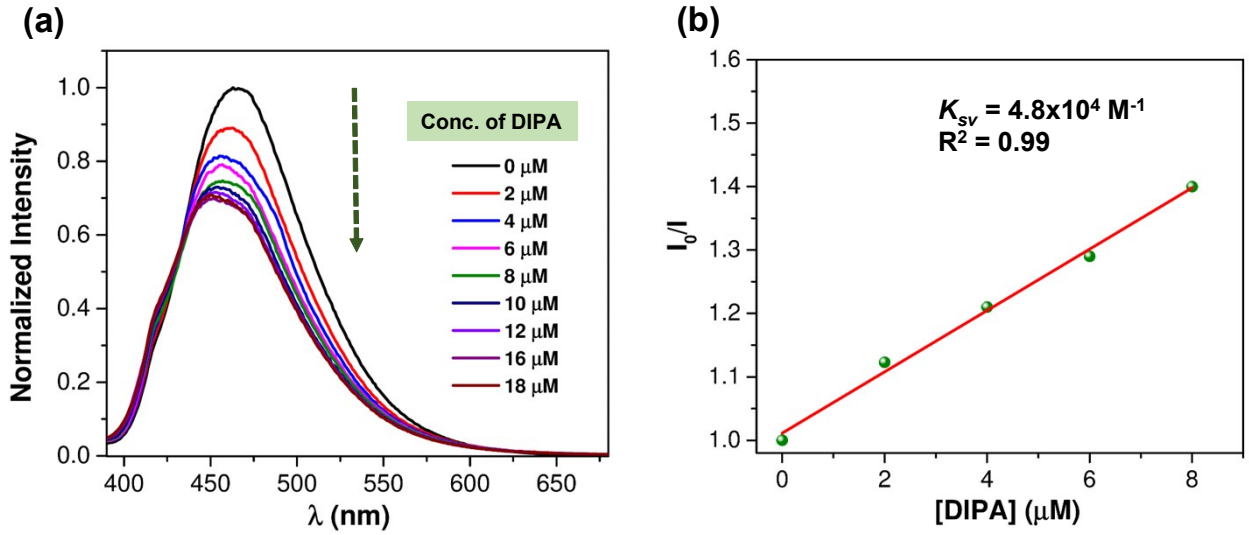

Fig. S4 (a) Quenching of the fluorescence of **Cd-BBI** with increasing concentration of DIPA. (b) Determination of the Stern–Volmer quenching constant.

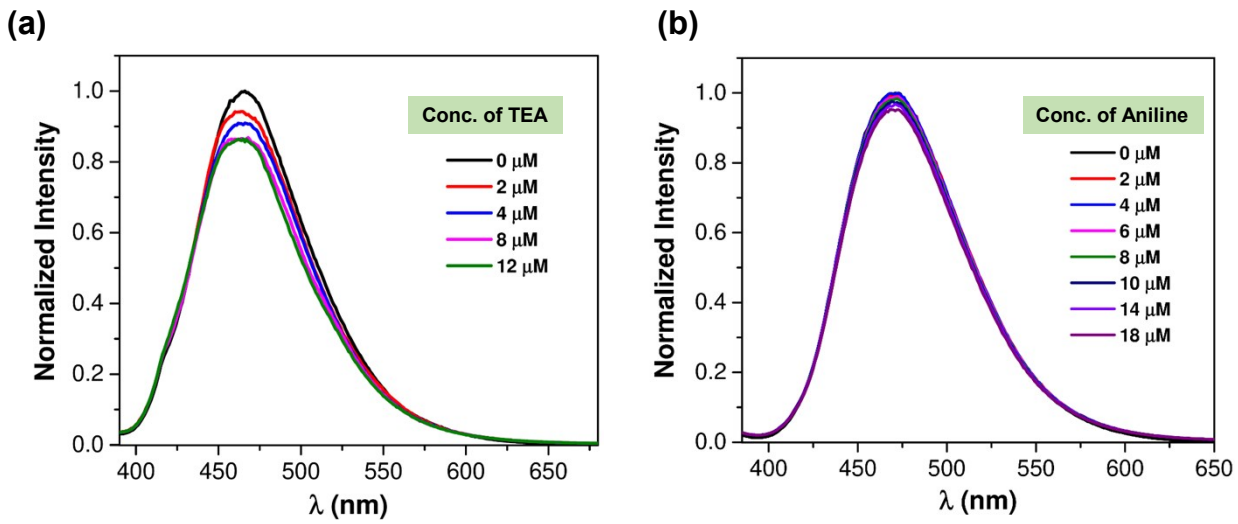

Fig. S5 Quenching of the fluorescence of **Cd-BBI** with increasing concentration of TEA (a) and aniline (b) in EtOH (λ_{ex} = 370 nm) at rt.

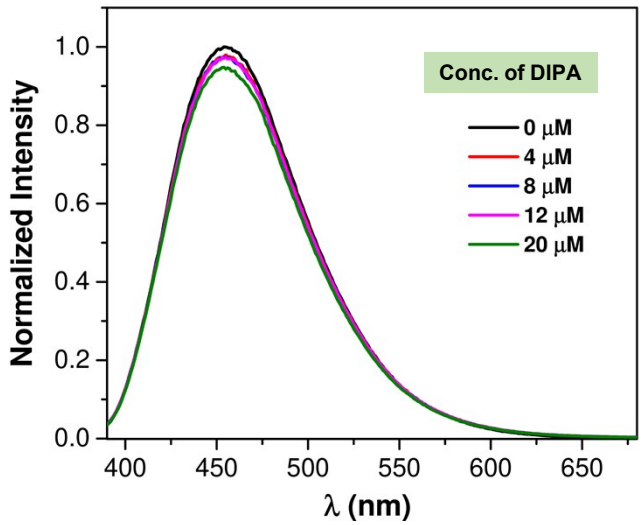

Fig. S6 Quenching of the fluorescence of tetraester **2** with increasing concentration of DIPA in EtOH (λ_{ex} = 370 nm).

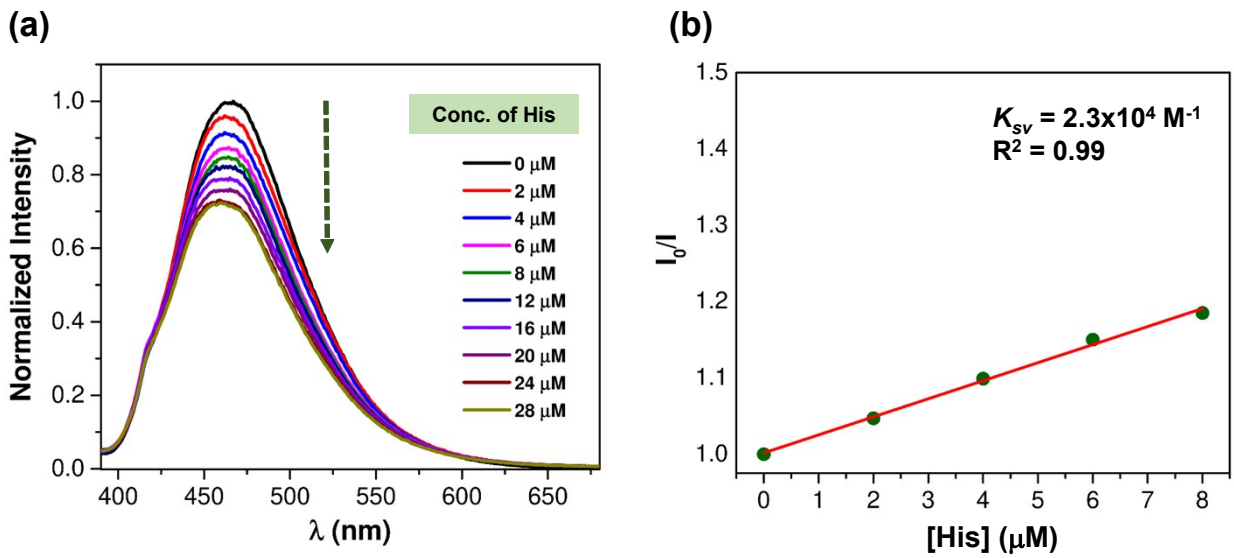

Fig. S7 (a) Quenching of the fluorescence of **Cd-BBI** with increasing concentration of His in EtOH (λ_{ex} = 370 nm). (b) Determination of the Stern–Volmer quenching constant.

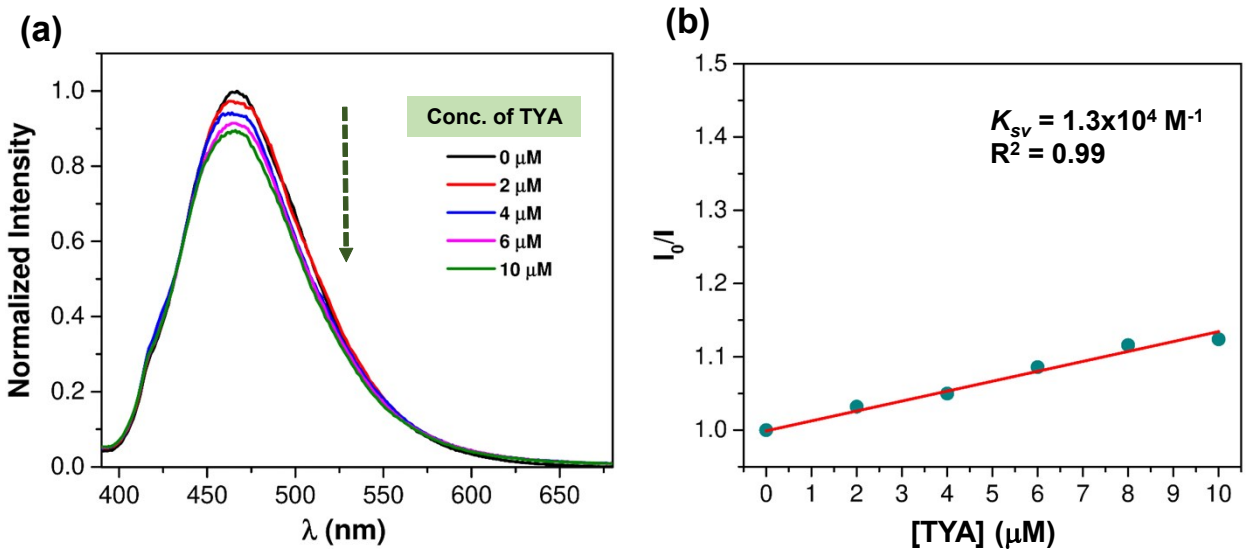

Fig. S8 (a) Quenching of the fluorescence of **Cd-BBI** with increasing concentration of TYA in EtOH (λ_{ex} = 370 nm). (b) Determination of the Stern–Volmer quenching constant.

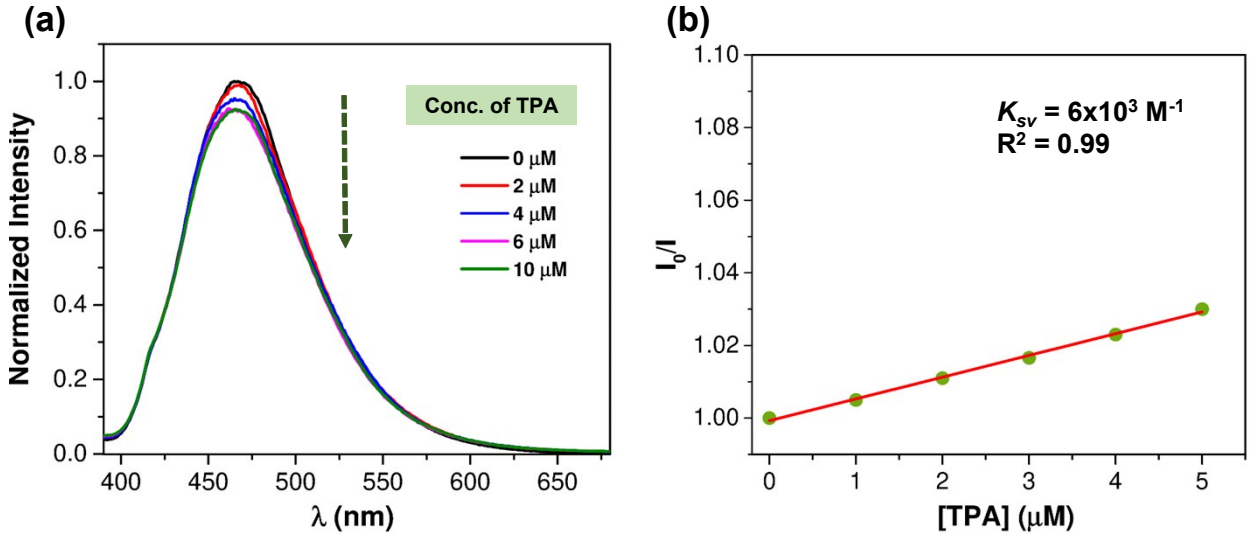

Fig. S9 (a) Quenching of the fluorescence of **Cd-BBI** with increasing concentration of TPA in EtOH (λ_{ex} = 370 nm). (b) Determination of the Stern–Volmer quenching constant.

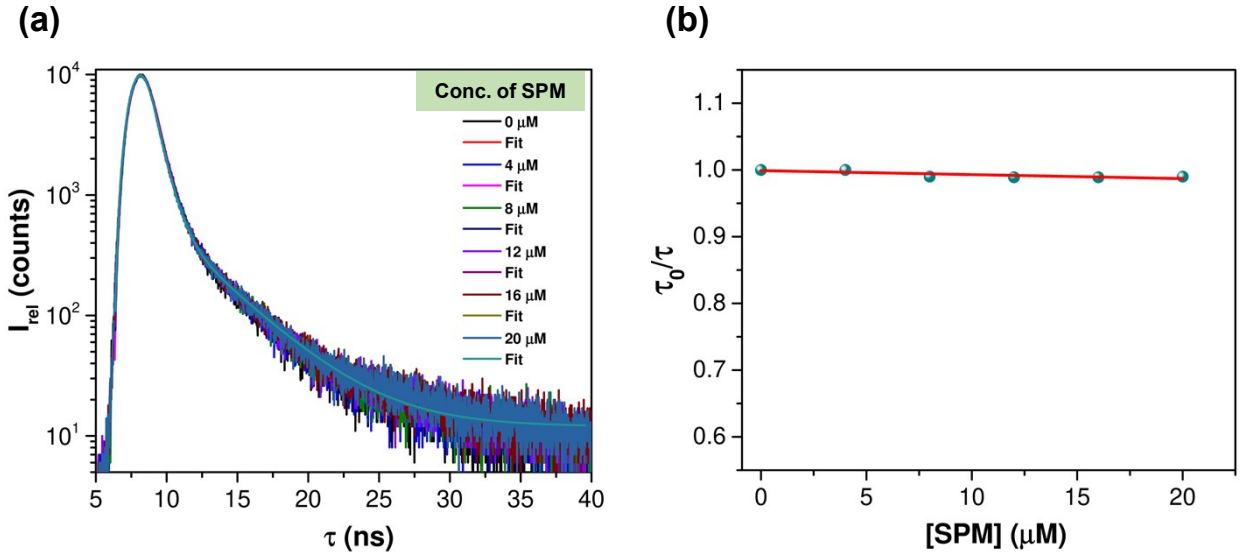

Fig. S10 (a) Time-resolved fluorescence quenching titration of **Cd-BBI** with increasing concentration of SPM in EtOH (λ_{ex} = 340 nm; λ_{em} = 470 nm). (b) A linear plot of (τ_0/τ) versus concentration of SPM**.**

Table S2 Fluorescence lifetime decay data of **Cd-BBI** for incremental addition of SPM.

S.No.	Conc. of SPM (μM)	τ_{avg} (ns) **Cd-BBI**	χ^2
1.	0	1.18	1.41
2.	4	1.18	1.41
3.	8	1.2	1.41
4.	12	1.21	1.38
5.	16	1.21	1.33
6.	20	1.21	1.35

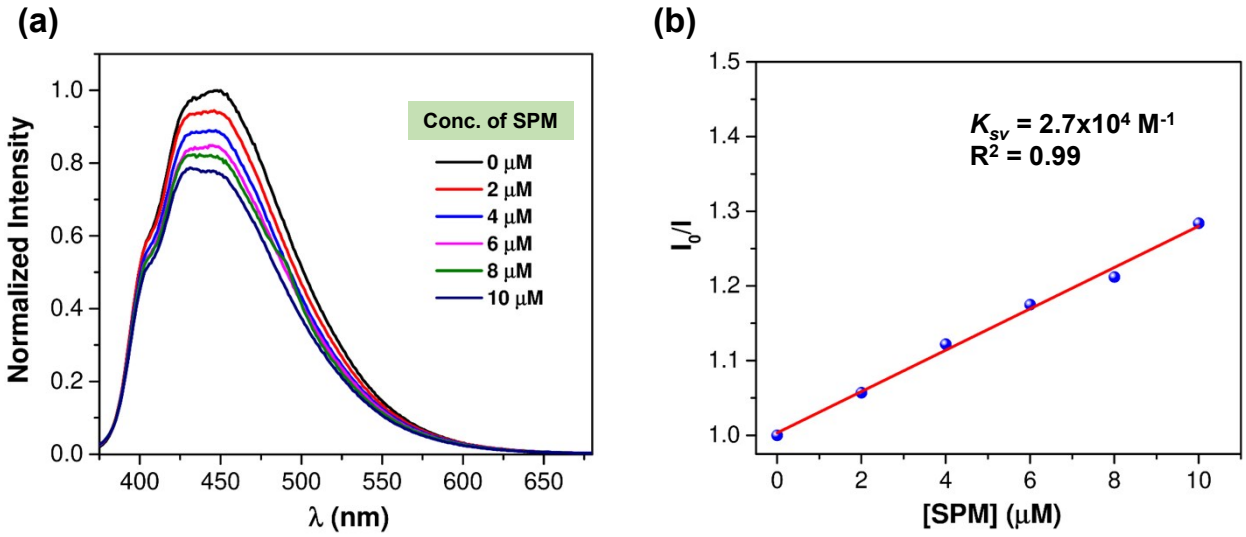

Fig. S11 (a) Quenching of the fluorescence of **H_4BBI** with increasing concentration of SPM in EtOH (λ_{ex} = 360 nm). (b) Determination of the Stern–Volmer quenching constant.

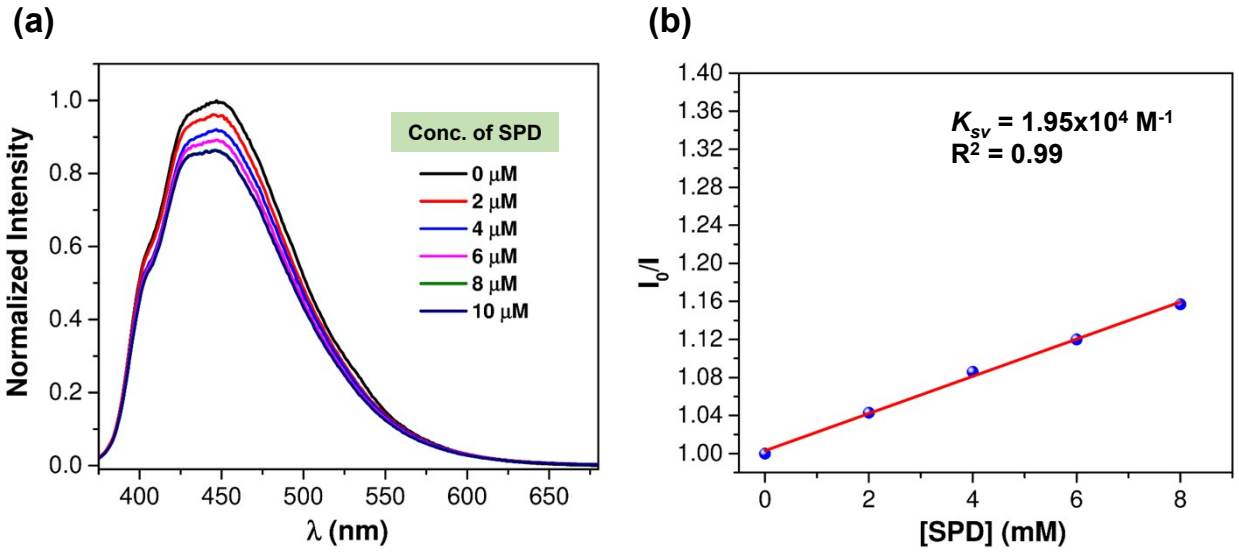

Fig. S12 (a) Quenching of the fluorescence of **H_4BBI** with increasing concentration of SPD in EtOH (λ_{ex} = 360 nm). (b) Determination of the Stern–Volmer quenching constant.

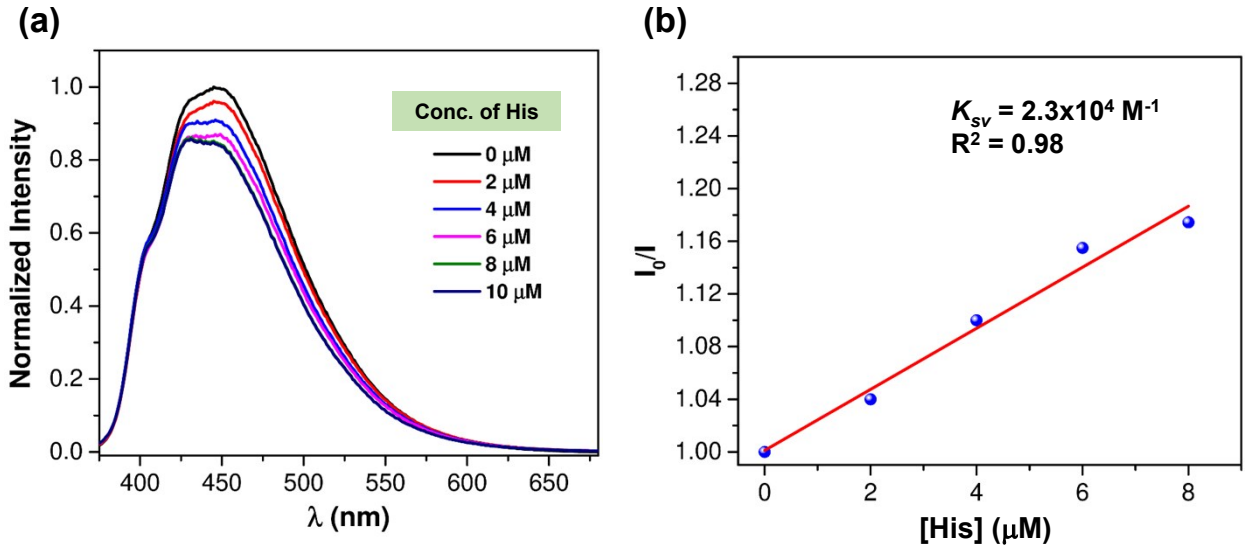

Fig. S13 (a) Quenching of the fluorescence of **H_4BBI** with increasing concentration of His in EtOH (λ_{ex} = 360 nm). (b) Determination of the Stern–Volmer quenching constant.

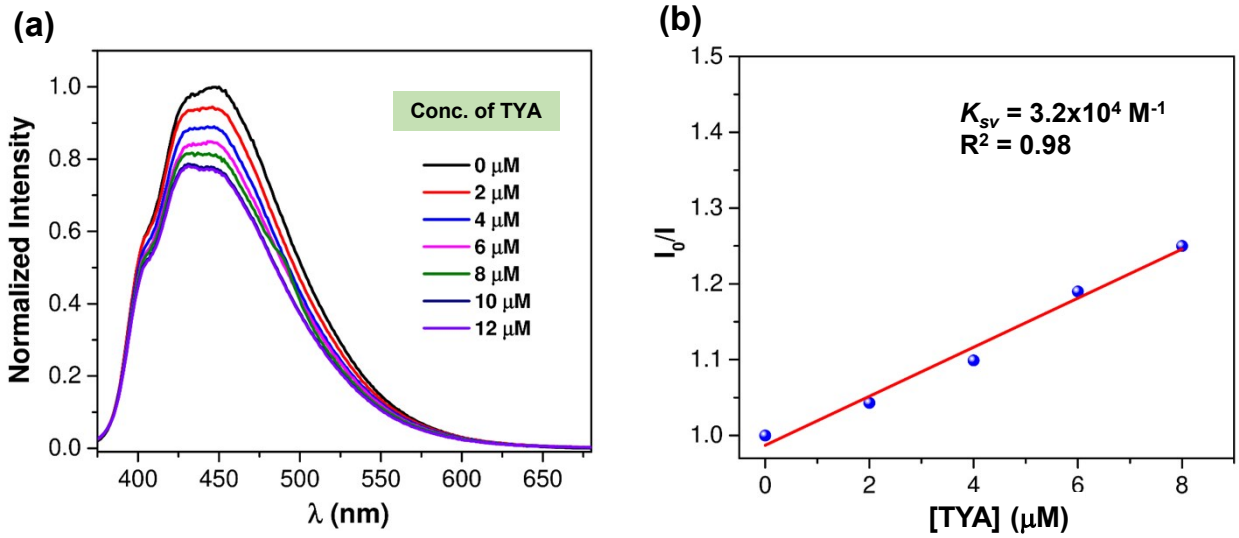

Fig. S14 (a) Quenching of the fluorescence of **H_4BBI** with increasing concentration of TYA in EtOH (λ_{ex} = 360 nm). (b) Determination of the Stern–Volmer quenching constant.

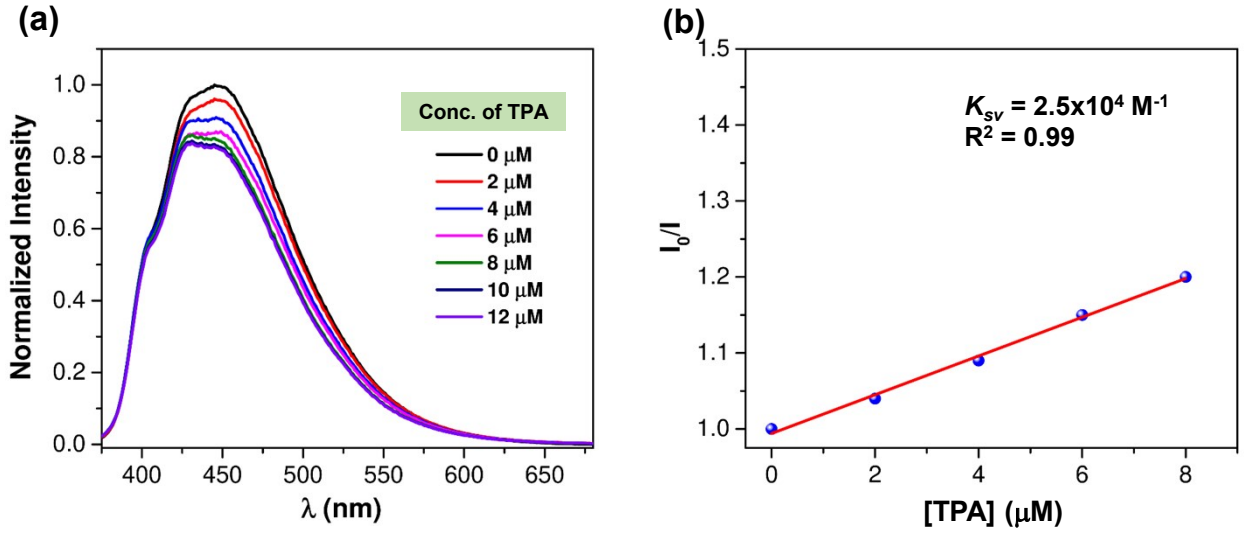

Fig. S15 (a) Quenching of the fluorescence of **H_4BBI** with increasing concentration of TPA in EtOH (λ_{ex} = 360 nm). (b) Determination of the Stern–Volmer quenching constant.

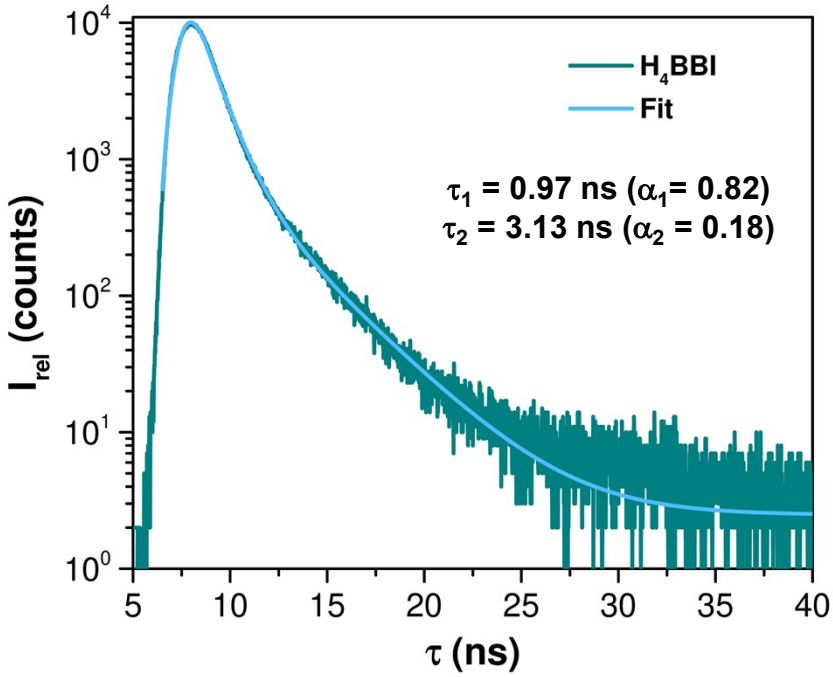

Fig. S16 Time-resolved fluorescence decay trace (λ_{ex} = 340 nm; λ_{em} = 450 nm) of **H_4BBI** in EtOH (1 μM) recorded using TCSPC. The monoexponential fitting ($\chi^2 \approx 1$) of the decay trace shows that the singlet lifetime ($^1\tau$) of **H_4BBI** is 1.36 ns.

Table S3 Fluorescence quenching data of **H_4BBI** ($^1\tau$ = 1.36 ns) for various biogenic amines in EtOH.

Quencher	K_{SV} (M^{-1})	k_q (10^{13} M^{-1} s^{-1})
SPM	2.7×10^4	1.9
SPD	1.9×10^4	1.4
His	2.3×10^4	1.7
TYA	3.2×10^4	2.3
TPA	2.5×10^4	1.8

Calculation of limit of detection

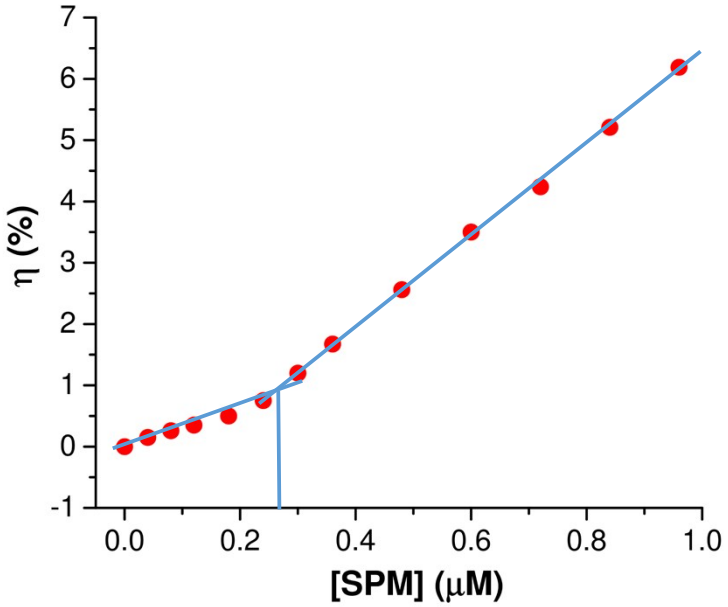

Fig. S17 Determination of the sensitivity limit of **Cd-BBI** for the detection of SPM. Notice that the limiting concentration was determined from the point of intersection of the two linear fits that are colored in blue.[2] The limiting concentration thus turns out to be 0.28 μM. The detection limit in ppb (i.e., μg/L) was calculated using the following equation:[3]

x (in ppb) = y (in μM) × molar mass of analyte/1000.

Given that the molar mass of SPM is 202.35, the detection limit in ppb = (0.28×202.35/1000) ppb ≈ 56 ppb.

Table S4 Comparison of sensing properties of **Cd-BBI** MOF with different SPM optical probes.

Probe	**Detection technique**	**Limit of detection**	**Reference**
Cd-BBI MOF	fluorescence quenching	0.28 μM	present study
Agarose-coumarin hydrogel (CB-AG)	fluorescence turn-on	6 μM	4
Perylene diimide–Cu^{2+} based nanoparticles	fluorescence quenching	90 pM	5
Naphthyl benzimidazolium	fluorescence quenching	6 nM	6
CdTe quantum dots coated amphiphilic thiophene copolymers	fluorescence turn-on	1.6 nM	7
AIEgen@cucurbit[7]uril based supramolecular system	fluorescence turn-off	1 μM	8
Ag−Au/AgCl nanohybrid	fluorescence turn-off	0.87 nM	9
Tyrosine functionalized Au-nanoparticles	fluorescence turn-on	636 pM	10
Copper complex of organic nanoparticles	UV-absorbance	36.2 nM	11
ctDNA gold nanoparticles	UV-absorbance	11.6 nM	12
PFBT-MI polymer-surfactant SDS self-assembled	fluorescence turn-off	0.33 μM	13
Pyrene derivative and squarine containing self-assembled system	fluorescence quenching	20 μM	14
Complexes of Pb(II), Cd(II), and Zn(II)	fluorescence turn-on	25 μM	15

References:

1 S. Pizarro, M. Gallardo, C. Leyton, E. Castro and F. Gajardo, *Spectrochim. Acta Part A Mol. Biomol. Spectrosc.*, 2015, **146**, 61–65.

2 A. Bajpai, A. Mukhopadhyay, M. Shivakumar, S. Govardhan and J. N. Moorthy, *IUCrJ*, 2015, **2**, 552–562.

3 A. Mukhopadhyay, V. K. Maka and J. N. Moorthy, *J. Org. Chem.*, 2016, **81**, 7741–7750.

4 R. R. Nair, S. Debnath, S. Das, P. Wakchaure, B. Ganguly and P. B. Chatterjee, *ACS Appl. Bio Mater.*, 2019, **2**, 2374–2387.

5 K. Kumar, S. Kaur, S. Kaur, G. Bhargava, S. Kumar and P. Singh, *J. Mater. Chem. B*, 2019, **7**, 7218–7227.

6 N. Tripathi, P. Singh, V. Luxami, D. Mahajan and S. Kumar, *Sens. Actuators B*, 2018, **270**, 552–561.

7 S. M. Tawfik, J. Shim, D. Biechele-speziale, M. Sharipov and Y. Lee, *Sens. Actuators, B*, 2018, **257**, 734–744.

8 G. Jiang, W. Zhu, Q. Chen, X. Li and G. Zhang, *Sensors Actuators B*, 2018, **261**, 602–607.

9 P. Kuo, C. Lien, J. Mao and B. Unnikrishnan, *Anal. Chim. Acta*, 2018, **1009**, 89–97.

10 K. A. Rawat, J. R. Bhamore, R. Kumar and S. Kumar, *Biosens. Bioelectron.*, 2017, **88**, 71–77.

11 S. Chopra, A. Singh, V. N. Singh and N. Kaur, *ACS Sustain. Chem. Eng*, 2017, **5**, 1287–1296.

12 J. Wang, Z. Lian, H. Zhi, Y. Fang and C. Zhi, *Talanta*, 2017, **167**, 193–200.

13 A. H. Malik, S. Hussain and P. K. Iyer, *Anal. Chem.*, 2016, **88**, 7358–7364.

14 J. Tu, S. Sun and Y. Xu, *Chem. Commun.*, 2016, **52**, 1040–1043.

15 J. T. Fletcher and B. S. Bruck, *Sens. Actuators B*, 2015, **207**, 843–848.

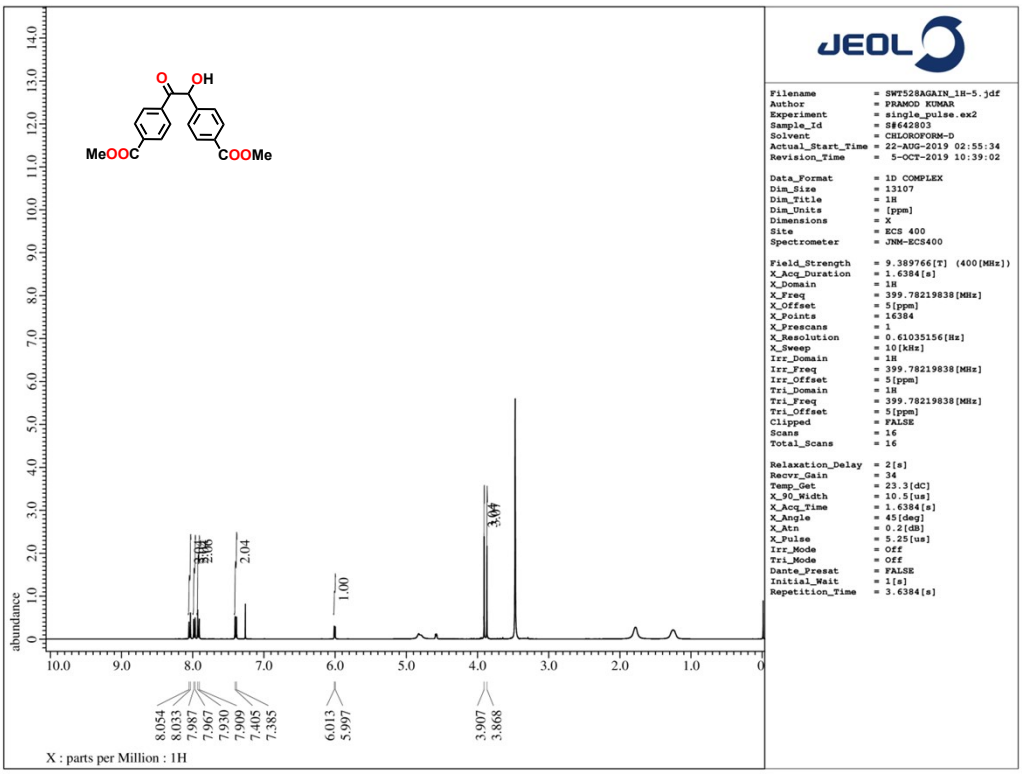

Fig. S18 ^{1}H NMR (400 MHz, $CDCl_3$) spectrum of dimethyl 4,4'-(2-hydroxyacetyl)dibenzoate.

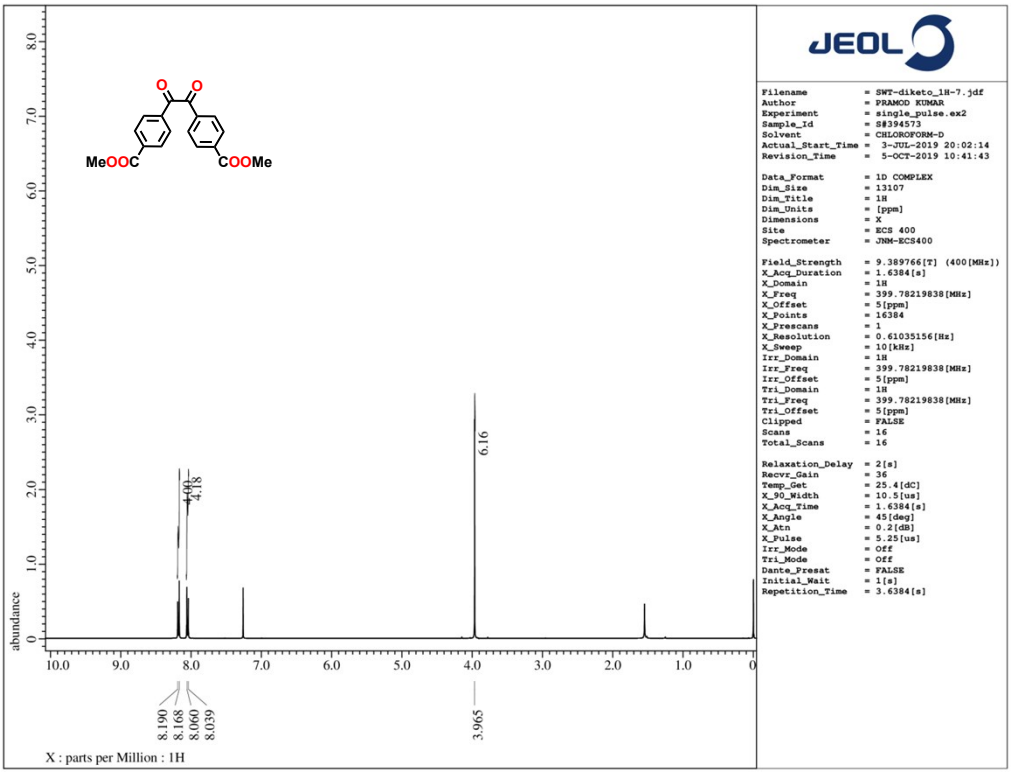

Fig. S19 ^{1}H NMR (400 MHz, $CDCl_3$) spectrum of diketodiester **1**.

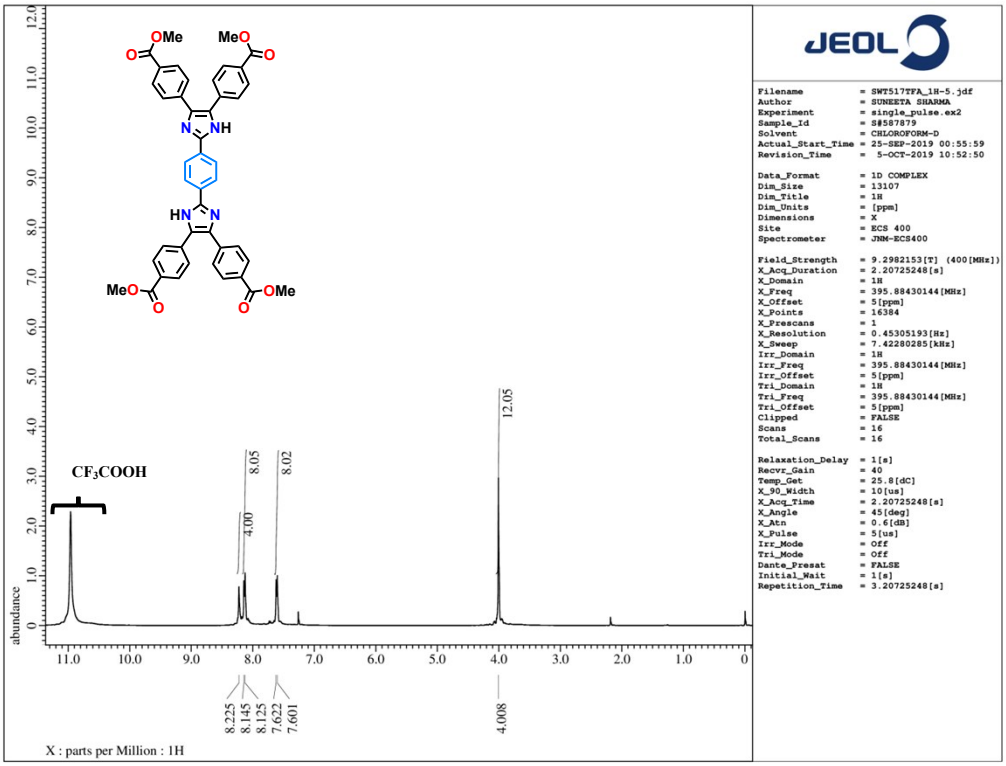

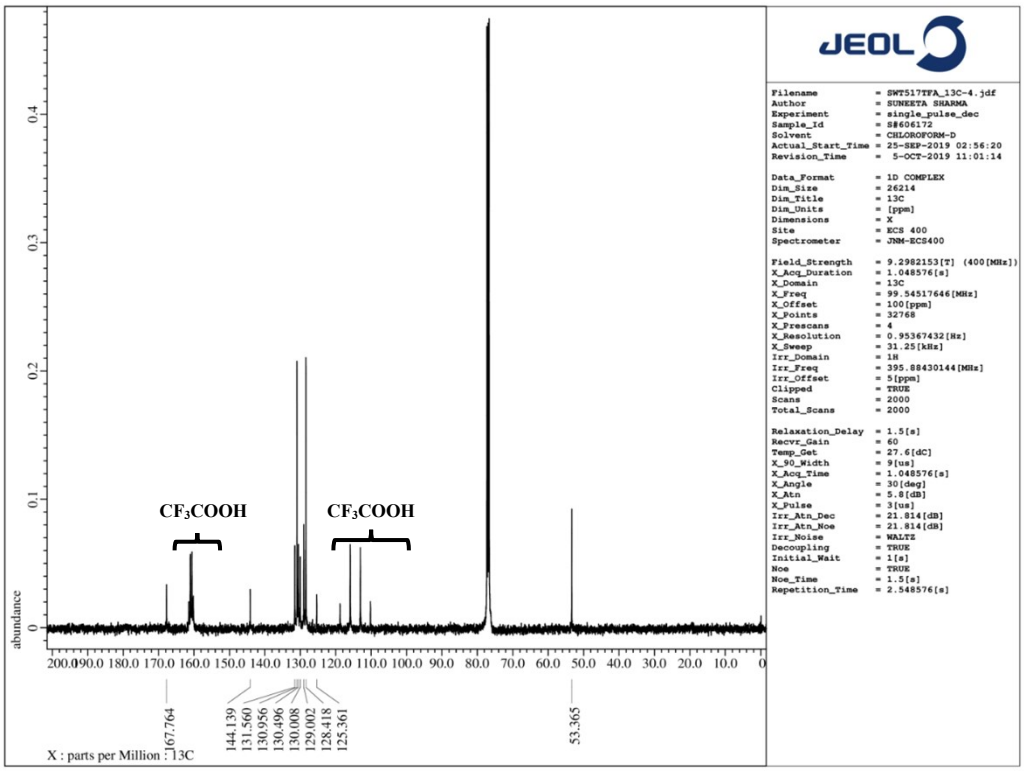

Fig. S20 ^{1}H NMR (400 MHz, $CDCl_3$) and ^{13}C NMR (100 MHz, $CDCl_3$) spectra in TFA of tetraester **2**.

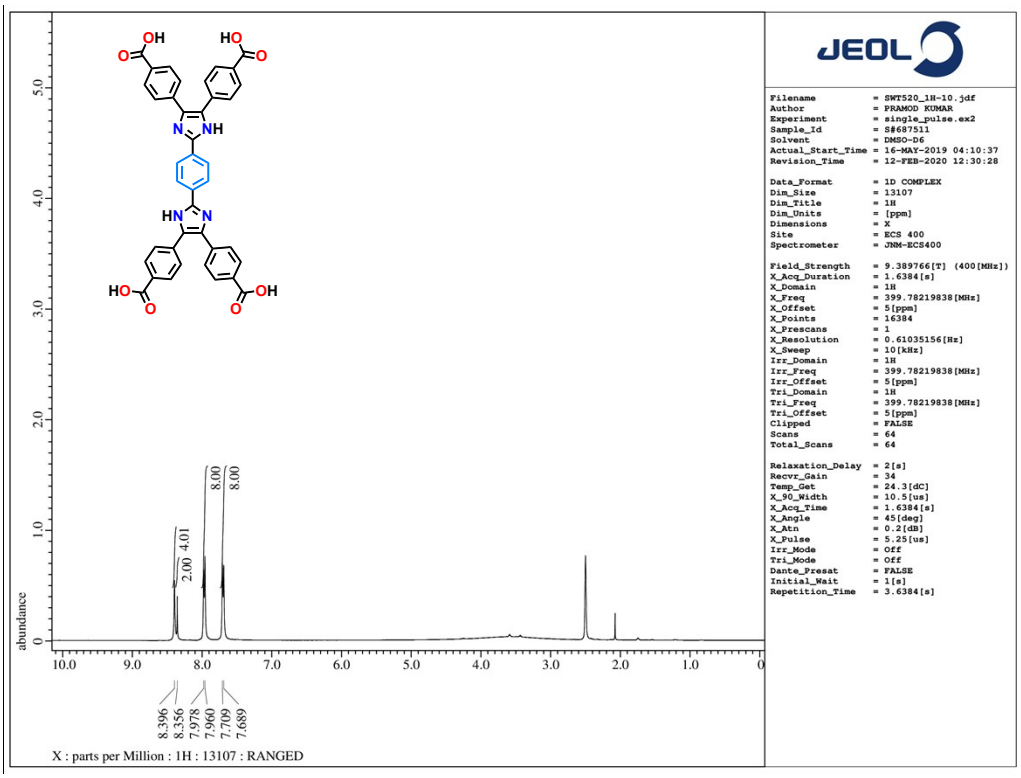

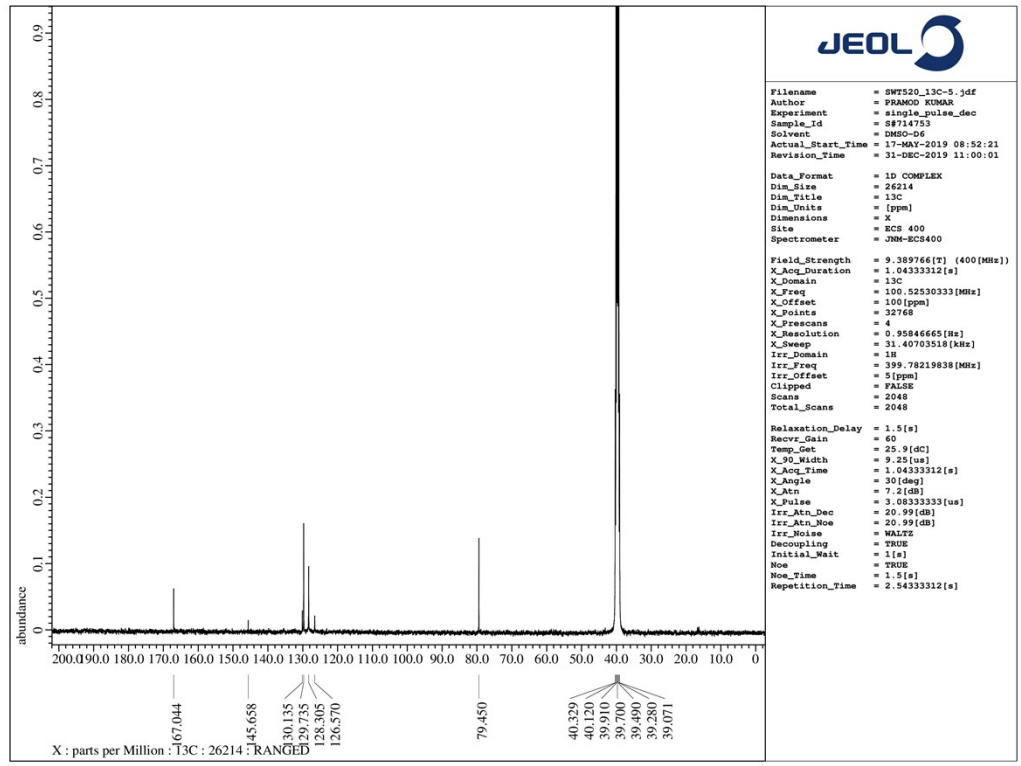

Fig. S21 ^{1}H NMR (400 MHz, DMSO-d_6) and ^{13}C NMR (100 MHz, DMSO-d_6) spectra of **H_4BBI**.